

## Simple coating method of carbonaceous film onto copper nanopowder using PVP as solid carbon source



Danee Cho<sup>a</sup>, Dahyun Choi<sup>a</sup>, Rajendra C. Pawar<sup>a</sup>, Sanggeun Lee<sup>b</sup>, Eric H. Yoon<sup>c</sup>,  
Tae-yoon Lee<sup>b</sup>, Caroline Sunyong Lee<sup>a,\*</sup>

<sup>a</sup> Division of Materials Engineering, Hanyang University, Ansan, Republic of Korea

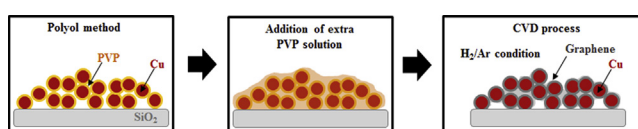
<sup>b</sup> School of Electrical and Electronic Engineering, Yonsei University, Republic of Korea

<sup>c</sup> Daechang Co. Ltd., Republic of Korea

### HIGHLIGHTS

- Carbonaceous film coating onto copper nanopowder.
- PVP as solid carbon source converted into carbonaceous film.
- Developed highly stable and well dispersed copper ink.

### GRAPHICAL ABSTRACT



### ARTICLE INFO

#### Article history:

Received 13 February 2014

Received in revised form

18 July 2014

Accepted 30 August 2014

Available online 30 September 2014

#### Keywords:

Metals

Chemical vapor deposition (CVD)

Heat treatment

Polymers

### ABSTRACT

A simple method of carbonaceous films coating onto copper (Cu) nanopowder is investigated with solid carbon source. Copper nanopowder was coated with carbonaceous films using chemical vapor deposition (CVD) using polyvinylpyrrolidone (PVP) as a solid carbon source via a polyol method. The process time and concentration of PVP solution during the CVD process were controlled to optimize the carbonaceous films coating while preventing nanoparticles agglomeration. From TEM and FESEM, it was found that the necking among copper particles was minimum with 3 min processing time at 900 °C using 30 wt% PVP solution. TG-DTA, XPS, FT-IR and Raman analysis confirmed the successful conversion of PVP into few nanometer-thick carbonaceous films layer coating on the surface of copper nanopowder without necking. Therefore, carbonaceous films coated copper nanopowder could be applied in copper ink application for better dispersion and high stability.

© 2014 Elsevier B.V. All rights reserved.

## 1. Introduction

Studies on the printed electronics have been growing with increasing interests in flexible device. Compared to photolithography, it is possible to pattern electronic circuit simultaneously without going through series of steps, such as deposition, patterning and etching. In particular, development of conductive ink for the application of printed electronics process is crucial. To make device using printed electronics process, dispersion stability

of conductive ink, the conductivity of the ink, low production costs, low sintering temperature, and durability, are the key factors to consider [1,2]. Especially, durability is one of the most important things necessary for commercialization because its initial properties of inks have to be maintained throughout its usage. The materials used for conductive ink have been silver, gold, and copper nano particles, which are mostly metal [3–5]. However, due to its high cost using noble metals, such as silver, and gold, copper inks have been studied extensively to replace them [2].

Copper is inexpensive and has good electrical and thermal properties, but it is easily oxidized in air. Therefore, studies have examined how to minimize this oxidation by reducing the exposure of the copper surface to oxygen for a wide range of

\* Corresponding author. Tel.: +82 31 400 4697; fax: +82 31 436 8146.

E-mail addresses: [sunyonglee@hanyang.ac.kr](mailto:sunyonglee@hanyang.ac.kr), [sunyong523@gmail.com](mailto:sunyong523@gmail.com) (C.S. Lee).

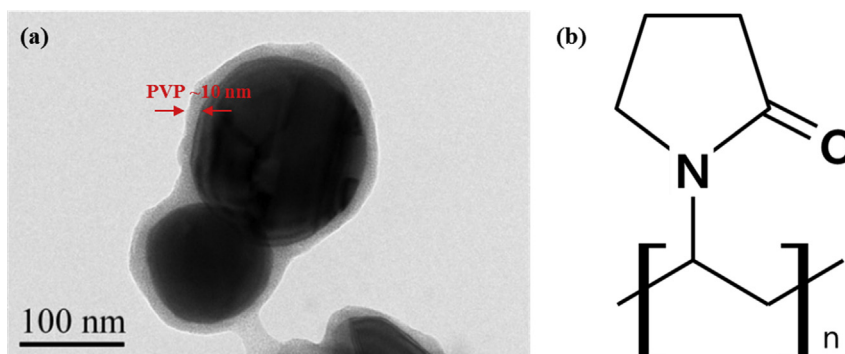


Fig. 1. (a) TEM image of PVP-coated copper nanoparticles and (b) the chemical structure of PVP.

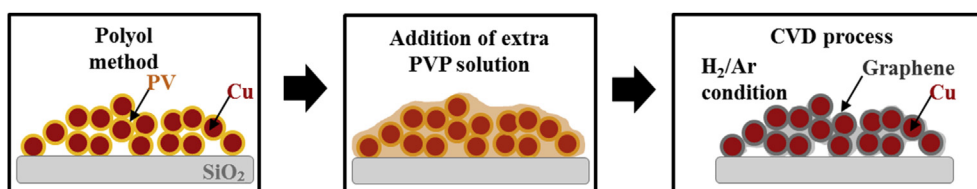


Fig. 2. Schematic of the experimental process.

applications. Various coatings can be used to protect against oxidation: metallic coatings [6–10], polymers [6,11–15], and coatings with thiol groups [7,16,17]. However, these coatings are limited by their properties. The noble metals used as coating materials are very expensive compared to that of copper. Protective coatings of conductive polymers and thiol groups can be used only on a limited number of materials, including copper, and the coating thickness can influence the properties of the core materials [18]. Moreover, the applicability of low-temperature sintering is limited because it is necessary to remove the polymer coating in inkjet printing applications through thermal and chemical treatment [18–20]. Therefore, studies have examined graphene as a protective coating to overcome the limitations of these other methods. Graphene has a higher electrical current density and higher thermal mobility than copper, and it is chemically stable because of its inert surface [21–23]. Recently, this inert material has been applied as a coating to protect against oxidation. In addition to preventing oxidation, graphene has excellent conductivity [6,18,24]. Studies have shown the

Table 1  
Experimental conditions.

No.	Condition	Temp.	Time	Heating rate	PVP solution
1	Air	500 °C	5 min	50 °C/min	–
2	Air	500 °C	5 min	50 °C/min	30 wt%
3	Air	600 °C	5 min	50 °C/min	30 wt%
4	Air	700 °C	5 min	50 °C/min	30 wt%
5	Air	800 °C	5 min	50 °C/min	30 wt%
6	Air	900 °C	5 min	50 °C/min	30 wt%
7	Ar/H <sub>2</sub>	900 °C	5 min	60 °C/min	30 wt%
8	Ar/H <sub>2</sub>	900 °C	3 min	60 °C/min	30 wt%
9	Ar/H <sub>2</sub>	900 °C	2 min	60 °C/min	30 wt%
10	Ar/H <sub>2</sub>	900 °C	1 min	60 °C/min	30 wt%
11	Ar/H <sub>2</sub>	900 °C	0 min	60 °C/min	30 wt%
12	Ar/H <sub>2</sub>	900 °C	3 min	60 °C/min	50 wt%
13	Ar/H <sub>2</sub>	900 °C	3 min	60 °C/min	70 wt%
14	Ar/H <sub>2</sub>	900 °C	3 min	60 °C/min	90 wt%

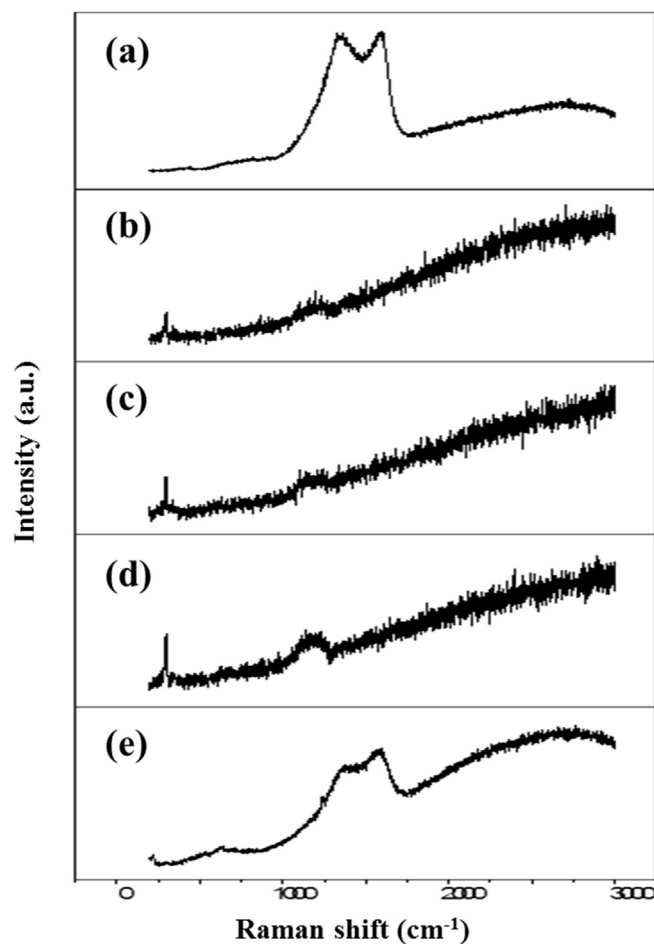


Fig. 3. Raman spectra of PVP-coated copper nanopowders after CVD at temperatures of (a) 900, (b) 800, (c) 700, (d) 600, and (e) 500 °C (Table 1, No. 2 through 6).

long-term oxidation prevention properties of graphene films grown on Cu films using chemical vapor deposition (CVD) [18,24]. CVD can be used to synthesize relatively high-quality graphene with a large area using a gas source at a relatively high temperature, to grow a graphene film on a surface using transition metals such as Ni, Cu, and Pd as catalysts [25–32]. However, because using a gas source for graphene synthesis involves temperatures over 1000 °C, the choice of transition metal catalysts is limited. By contrast, graphene film can be coated on a Cu surface using a polymer as a solid carbon source instead of using a gas source. It has been reported that carbonaceous film could be prepared using a variety of polymers which consist of carbon chains, such as amorphous carbon, PMMA, PS and PAN [33–37]. This method has the advantage of also blocking heat transfer to the Cu surface, which minimizes necking of the Cu powder while forming the carbonaceous film coating. Moreover, the process temperature can be reduced by using a solid carbon source [36–38].

In the present work, authors have explored a simple method of forming carbonaceous films coating onto copper nanopowder using PVP as a solid carbon source. Since PVP was formed on the surface of Cu nano powder during Cu powder synthesis as a part of polyol process, it is very simple to transform PVP coating to carbonaceous film. PVP coated copper nanoparticles via polyol process can prevent Cu nanoparticles from oxidation during its synthesis. Additionally, particle size distribution of copper nanopowders was well controlled using polyol process [39,40]. At low temperature, it is possible to convert PVP into

carbonaceous films because PVP coating layer formed on the copper particles, also has a relatively low decomposition temperature (140–500 °C) and vinyl based polymer may be applied to the solid carbon source of carbonaceous films [36,41–43]. The PVP layer on the copper nano powders was converted into carbonaceous films using CVD, without any gas source, and oxidation rate of copper nanopowder is minimized. Ink or paste for electrical materials in this research would be the possible application since carbonaceous films, considered to be one of the ideal materials with chemical stability, are formed directly on the spherical copper particle [24].

Process parameters, such as the CVD process time and concentration of PVP solution, were optimized to allow formation of carbonaceous films coating and preventing the agglomeration of nano powders.

## 2. Experimental details

Copper nano powders (~100 nm in diameter) were synthesized using the polyol method and coated with PVP as shown in Fig. 1 [44]. After its synthesis, solution of copper nano powders was centrifuged two times in methanol to remove remained diethylene glycol in polyol method. Then, nano powders were dispersed in PVP solution for coating (PVP, chloroform, and dimethylformamide in a 1:5:5 weight ratio) at different concentrations varied from 30 to 90 wt%. Finally, PVP solution with dispersed nano powders was deposited on a  $1.5 \times 1.5\text{-cm}^2$  SiO<sub>2</sub> substrate. Whole process mentioned above was conducted under Ar in a glove box to

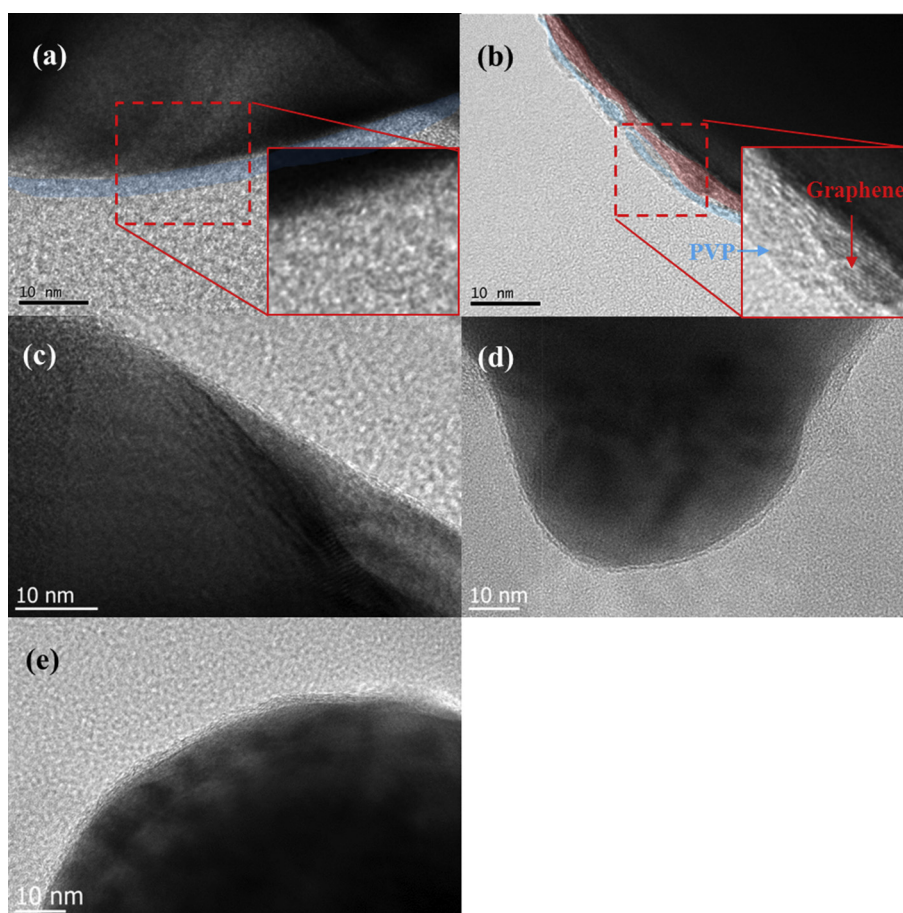


Fig. 4. TEM images of copper nanopowders after CVD for process times of (a) 0, (b) 1, (c) 2, (d) 3, and (e) 5 min (Table 1, No. 7–11).

prevent oxidation. After this, the conversion of PVP into a carbonaceous films layer made in CVD by varying the temperature, time, and concentration of extra PVP solution. During this process, Ar and H<sub>2</sub> gases were maintained at 50 sccm each. Fig. 2 shows a schematic of the experimental process, and the process variables during the CVD process are summarized in Table 1. TEM was used to observe the crystallinity and the thickness of the layers coating on the copper nano powders after the CVD process, and necking of the powders was examined using SEM. Finally, TG-DTA, XPS, FT-IR and Raman analysis were used to determine whether the PVP coating on the Cu powder had been converted into carbonaceous films.

### 3. Results and discussion

#### 3.1. Effect of process temperature

PVP coated Cu nano powders were processed at a temperature from 500 to 900 °C in air atmosphere and subjected to Raman analysis to determine PVP conversion into carbonaceous films (Fig. 3). The process conditions are listed in Table 1. All of Raman spectra showed copper oxide peaks at 296, 343, and 634 cm<sup>-1</sup>, due to the exposure of copper to air [45,46]. The spectrum of the sample processed at 500 °C showed peaks similar to those of amorphous carbon, while a peak for polymeric amorphous carbon was found for the temperature higher than 800 °C [48]. Finally, the

Raman spectrum at 900 °C showed the G band (~1580 cm<sup>-1</sup>) and 2D band (around ~2680 cm<sup>-1</sup>) corresponding to carbonaceous films. Additionally, it exhibits a high-intensity D band at 1356 cm<sup>-1</sup>, indicated the presence of many defects in formed carbonaceous films, possibly due to formation of carbonaceous films from PVP [26]. Therefore, it is optimized that 900 °C is the suitable temperature for conversion of PVP into carbonaceous films.

#### 3.2. Effect of process time

After optimization of temperature further we studied the CVD process time because it can affect on amount of necking among copper nano powders. Here, the term “necking” refers to agglomeration among Cu nano powders, leading to coarsening and sintering. Since carbonaceous film coating on individual Cu nano powder is a key process, minimizing necking among Cu nano powders, is crucial in this process. Fig. 4 show TEM images of copper nanopowder using CVD process times from 0 to 5 min at 900 °C. It is clearly seen that the thicknesses of coating layer did not vary noticeably with the processing time. However, the conversion to carbonaceous films is completed at processing times from 2 to 5 min. Initially, PVP remained as it is (Fig. 4(a)) and then it starts to convert into carbonaceous films slowly (Fig. 4(b)), leaving behind small amount of PVP. The different coating structures shown in the inset of Fig. 4(b) confirm the presence of

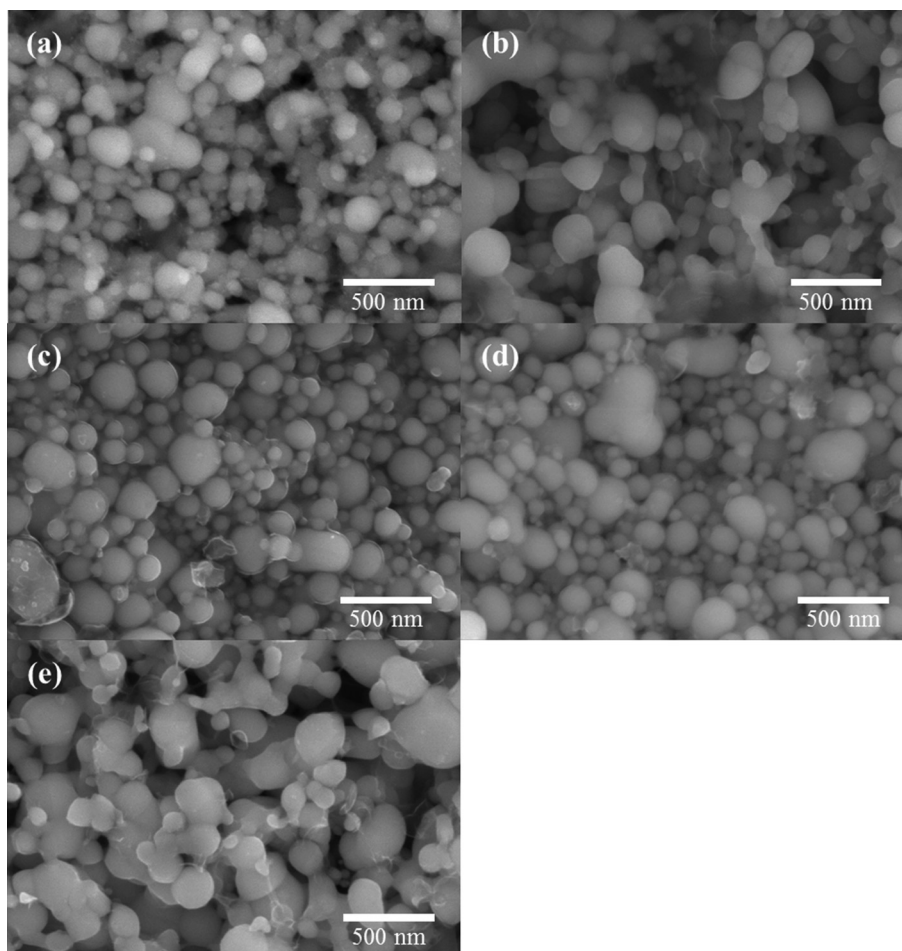
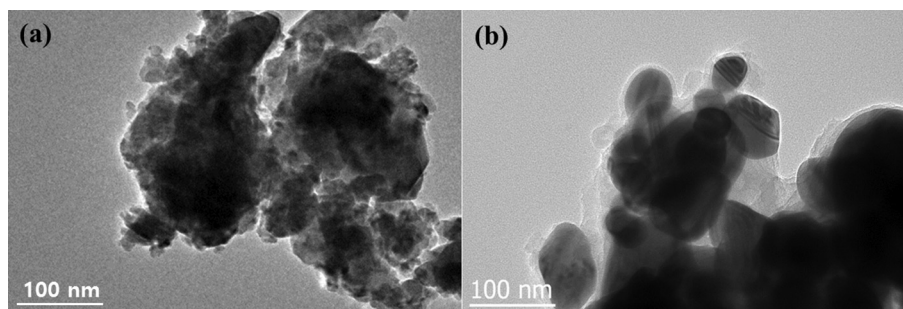


Fig. 5. SEM images of copper nanopowders after CVD for process times of (a) 0, (b) 1, (c) 2, (d) 3, and (e) 5 min (Table 1, No. 7 through 11).



**Fig. 6.** TEM images of copper nanopowders after CVD using the process specified in No. 1 and 2 (Table 1) (a) without and (b) with extra PVP solution.

residual PVP. Therefore, the minimum process time required to convert the PVP into carbonaceous films was 2 min. A 5-min. process resulted in necking among the copper nanopowder particles (Fig. 5 (e)). Hence, the optimum CVD process time to minimize the necking of the copper nanopowder and allow the complete conversion of PVP into carbonaceous films was 2–3 min.

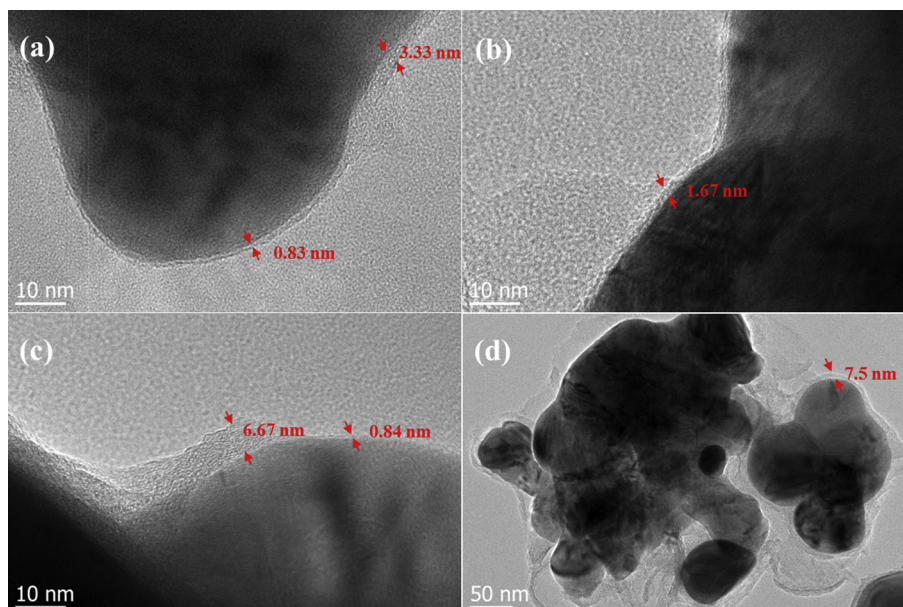
### 3.3. Effect of extra PVP solution

Fig. 1(a) shows a TEM image of a 10-nm-thick PVP layer on the copper nanopowder that formed as a result of the polyol process. Fig. 1(b) shows the chemical structure of PVP. Upon increasing the temperature, PVP dissociates into carbonaceous films via bond breakage. However, increasing the temperature to promote conversion into carbonaceous films also increased the probability of Cu nanopowder agglomeration before the PVP turns into carbonaceous films. Therefore, extra 30 wt% PVP solution was added to minimize agglomeration of the copper nanopowders before the PVP was converted to carbonaceous films. Fig. 6 shows TEM images of copper powders with and without extra PVP solution. Without the extra PVP solution (Fig. 6(a)), the copper nanopowders oxidized and agglomerated. With the extra PVP solution (Fig. 6(a)), the

copper nano powders were not oxidized and the particles remained separated. Therefore, additional PVP solution can protect the copper nano powders from oxidation and agglomeration at high temperature and in air. Due to its low processing temperature (500 °C), however, not all of the PVP on the copper nano powders was converted into carbonaceous films, leaving residual organic PVP.

Therefore, we examined the effect of varying the PVP concentration from 30 to 90 wt% (Fig. 7). In general, the thickness of the carbonaceous films layer on the copper nano powders increased with PVP concentration. With 30 wt% PVP (Fig. 7(a)), the average thickness of the carbonaceous films layer was less than 3 nm. The thinnest part of the carbonaceous films coating was roughly 0.83 nm thick. Because a single layer of carbonaceous films is about 0.35 nm thick, there were only two layers of carbonaceous films. In comparison, when 90 wt% PVP was added, the average thickness of the carbonaceous films layer was approximately 7.5 nm and there were traces of carbonaceous films sheets around the copper nano powders.

SEM was used to determine necking behavior among the powder particles (Fig. 8). Without extra PVP solution, extensive coarsening of Cu nano powders was observed, as shown in Fig. 8(a). With 30 and 50 wt% of PVP solutions (Fig. 8(b) and (c)), the copper nano



**Fig. 7.** TEM images of copper nanopowders after CVD with extra PVP (Table 1, No. 8, 12, 13 and 14): (a) 30, (b) 50, (c) 70, and (d) 90 wt% PVP solution added.

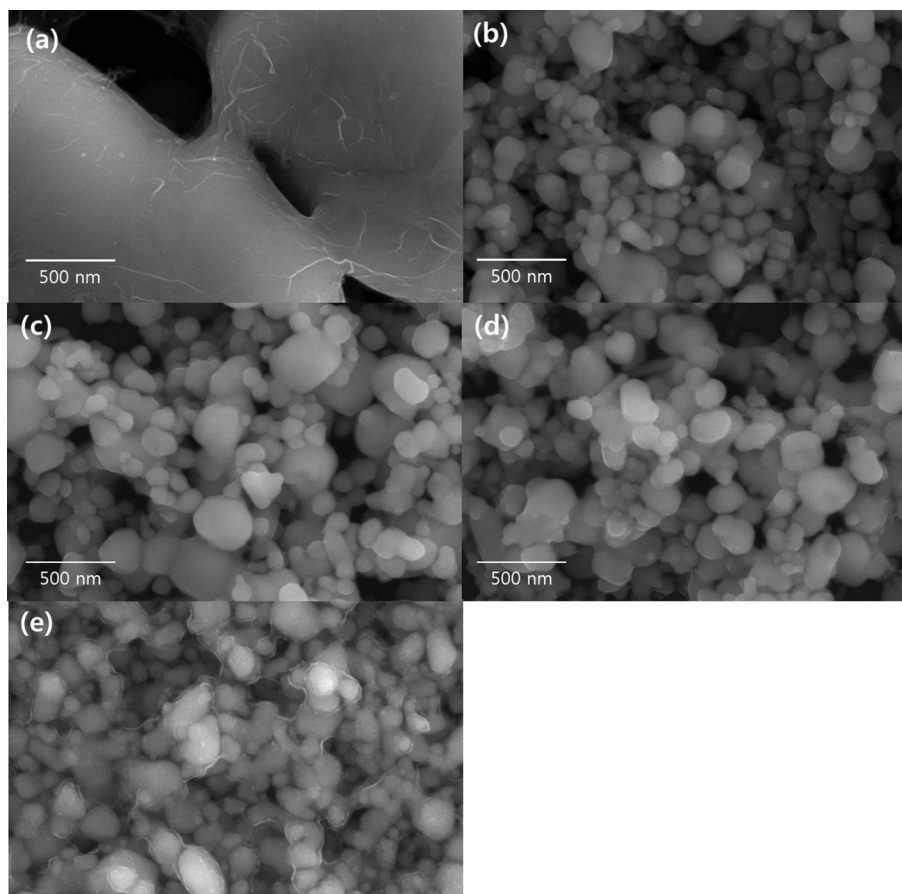


Fig. 8. SEM images of copper nanopowders after CVD (a) without PVP solution and with (b) 30, (c) 50, (d) 70, and (e) 90 wt% PVP solution added (Table 1, No. 8, 12, 13, and 14).

powders were not connected to each other. With 70 and 90 wt% PVP solutions (Fig. 8(d) and (e)), most of the copper nano powders were surrounded by a thick carbonaceous films coating with no particle agglomeration. Therefore, increasing the PVP concentration leads to a thick PVP coating.

Raman spectroscopy was used to show that all of the PVP was successfully converted into carbonaceous films (Fig. 9). The spectra showed major Raman peaks for carbonaceous films: a G band at  $\sim 1580\text{ cm}^{-1}$ , 2D band at  $\sim 2670\text{ cm}^{-1}$ , and D band at  $\sim 1350\text{ cm}^{-1}$  [22,47–51]. However, the peak for the D band indicates defects in the carbonaceous films [46]. Moreover, as the amount of PVP was increased to 90 wt%, the Raman peak showed features of

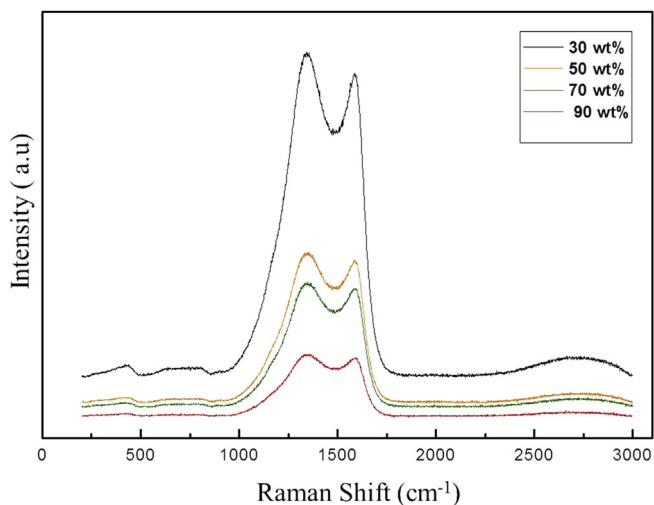


Fig. 9. Raman spectra of copper nanopowders after CVD with the extra PVP solution specified (Table 1, No. 8, 12, 13 and 14).

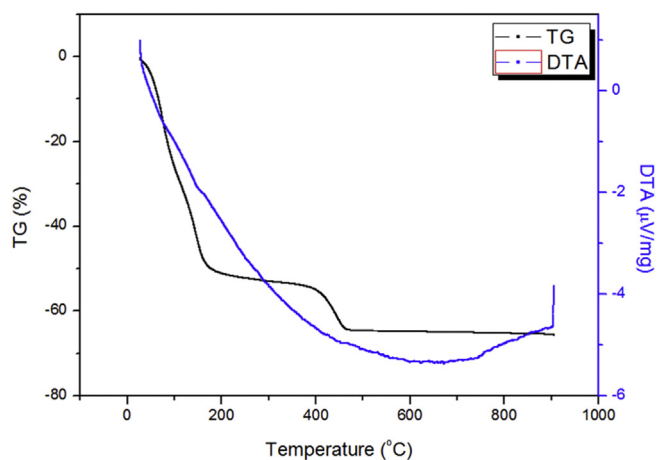


Fig. 10. TG-DTA analysis of PVP-coated copper nanopowders (Table 1, No. 8).

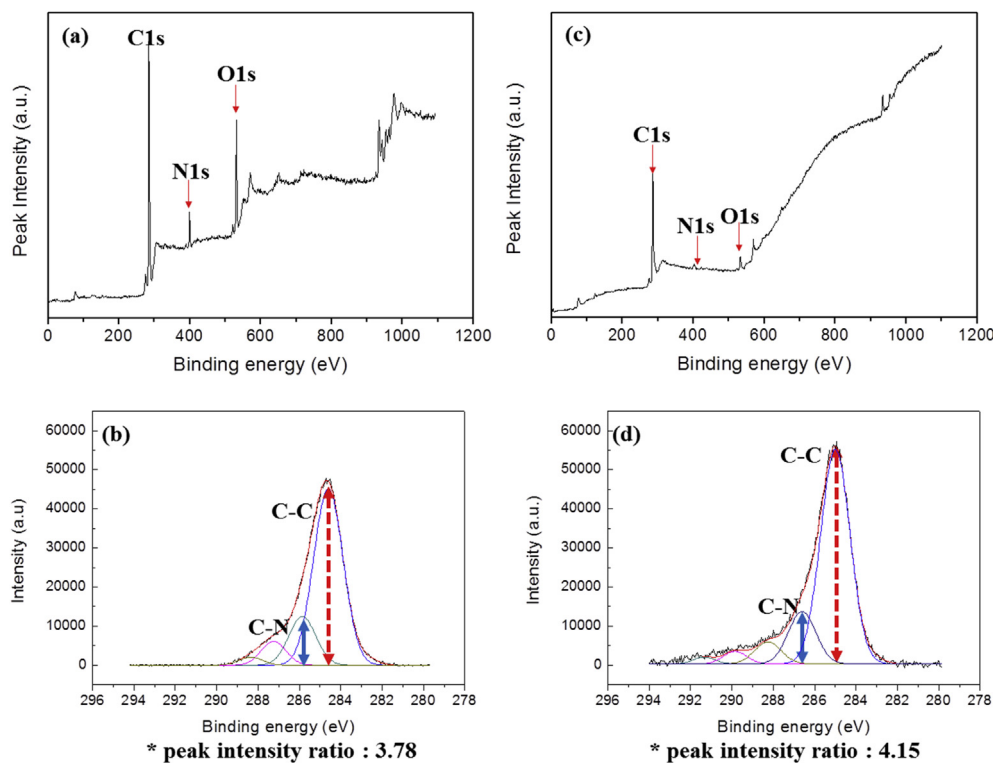


Fig. 11. XPS analysis of PVP-coated copper nanopowders with 30 wt% PVP solution: (a) and (b) before CVD process, (c) and (d) after CVD process (Table 1. No. 8).

amorphous carbon [52], indicating that not all of the PVP coating was converted into carbonaceous films. While increasing the PVP concentration reduced agglomeration or necking among copper nano powders due to its thick coating formed, not all of the PVP was converted into carbonaceous films. Adding 30 wt% PVP solution was the optimum amount for forming a thin carbonaceous films coating on the copper nano powders, while minimizing necking among the Cu nanopowder particles during the CVD process.

#### 3.4. Confirmation of the conversion of PVP into carbonaceous films

To determine exact amount of carbon present on the Cu nano particle during PVP conversion into carbonaceous films, TG-DTA analysis of PVP coated Cu nano powders was performed as

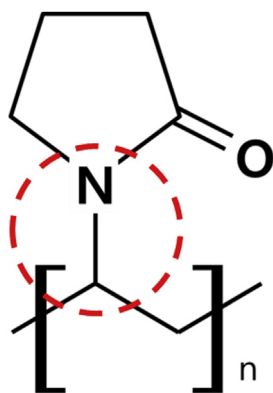
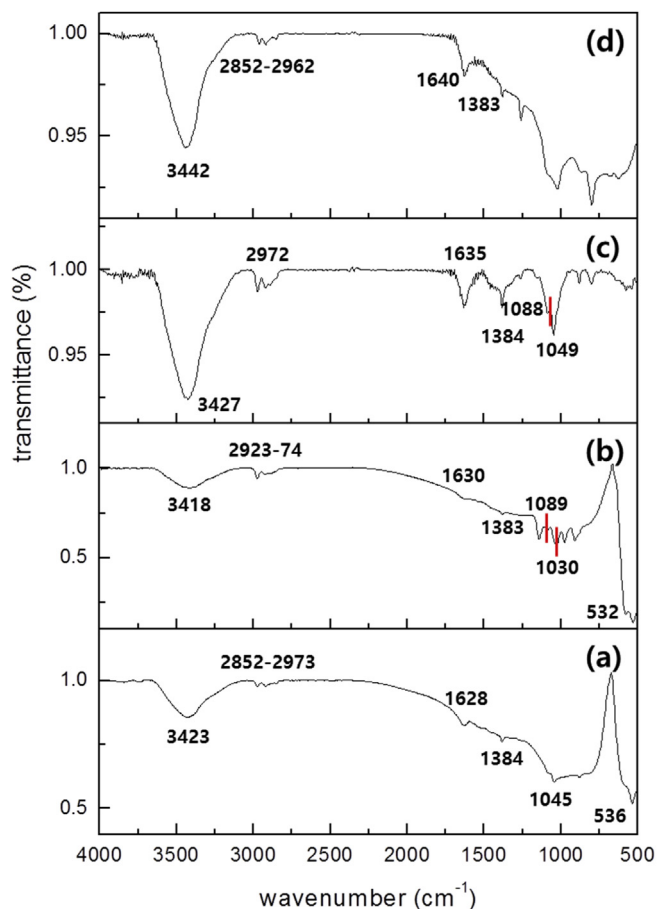


Fig. 12. The C–N bond in PVP.

shown in Fig. 10. It is observed that the first change in slope of the curve during temperature interval between 25 and 164 °C is rapid due to its evaporation of chloroform and dimethylformamide. In their second reducing slope, the mass of sample decreased about 5% between 164 and 407 °C, indicating decomposition of PVP [41–43]. Finally, the mass of the sample decreased by 10% until 468 °C. Therefore, TG-DTA analysis showed that the polymer chains in PVP decomposed successfully to amorphous carbon chain during CVD process.

To ensure that the PVP on the surface of the Cu nanopowder was successfully reduced to carbonaceous films during the CVD process, XPS was used to analyze the PVP-coated copper nanopowders and the copper nanopowders after CVD process (Table 1, sample no. 8) (Fig. 11). The XPS N1s and O1s peak intensities of the Cu nanopowders tended to decrease after the CVD process (Fig. 11(a) and (c)). This means that the CVD process broke the carbon–nitrogen (C–N) bonds in the PVP structure (Fig. 1(b)). Fig. 11(b) and (d), specifically shows the ratios of the peak intensities between C–C and C–N bonds, which were used to monitor the conversion of PVP to carbonaceous films. The peak intensity ratio for the PVP-coated Cu nanopowder increased from 3.78 (Fig. 11(b)) to 4.15 (Fig. 11(d)) before and after the CVD process, confirming that the C–N bonds in PVP were broken, leaving only the C–C bonds of PVP to be converted into hybridized  $sp^2$  carbon bonds (Fig. 12) [53].

FT-IR analysis was used to prove the composition of those samples. For FT-IR analysis, 4 samples (Table 1, No. 1, 6, 8, 14) were selected for comparison as shown in Fig. 13. The basic hydroxyl group  $\text{OH}^-$  at  $3420\text{--}3440\text{ cm}^{-1}$  [54] and CH stretching vibrations at  $2852\text{--}2973\text{ cm}^{-1}$  [55,56]. were observed for all samples. The spectrum of PVP has the peak of CN bonding at  $1384\text{ cm}^{-1}$  [57] and C–N bonding at  $1030\text{--}1045\text{ cm}^{-1}$  [58]. All the samples showed those peaks for PVP and these results matched XPS



**Fig. 13.** FT-IR analysis of PVP-coated copper nanopowders under the following CVD process conditions: (a) Table 1, No. 1, (b) Table 1, No.6, (c) Table 1, No. 8 and (d) Table 1, No. 14.

analysis where various amount of C–N bonding was present before and after CVD process. Moreover, all samples had C–C bonding at 1628–1640  $\text{cm}^{-1}$ , proving transformation of carbonaceous film [59]. Among those samples, Figure (c) shows the strongest intensity at 1635  $\text{cm}^{-1}$ , indicating successful conversion to carbonaceous film. Samples no.1 and no.6 shown in Fig. 13(a) and (b), which were processed in air, showed the copper oxidation (CuO) peak around 500  $\text{cm}^{-1}$  [60]. However, two samples

(no.6 and no.8) processed under almost the same condition but different atmospheres (Fig. 13(b) and (c)), showed C–O bonding at 1088  $\text{cm}^{-1}$  [59] but the sample processed (Table 1, No. 6) in air, had higher intensity of C–O peak than that of the sample processed under Ar/H<sub>2</sub> (Table 1, No. 8) atmosphere. Moreover, sample No. 14 (Fig. 13(d)) with excessive amount of PVP solution showed its high intensity peaks for CN or C–N bonding peak. This excessive PVP solution reduced the oxidation of copper particle where copper oxidation (CuO) peak around 500  $\text{cm}^{-1}$  and C–O bonding at 1088  $\text{cm}^{-1}$  were not observed. However, the intensity of C–C bonding at 1628–1640  $\text{cm}^{-1}$  was relatively low compared to that of sample no.8 (Fig. 13(c)). Based on these comparisons, sample no. 8 (Fig. 13(c) shows the most successful conversion of carbonaceous film from PVP with relatively small amount of PVP left.

Raman spectra for copper nano powders with the PVP coating before and after the CVD process were provided in Fig. 14. It is seen that the peak for copper powder were observed at ~565, 624, and ~1092  $\text{cm}^{-1}$ , and there is no peak related to carbonaceous films (Fig. 14(a)) [46]. However, after the CVD process (Fig. 14(b)), peaks corresponding to carbonaceous films at ~1580 and 1680  $\text{cm}^{-1}$ , were observed [47–51]. Therefore, the reduction of PVP to carbonaceous films after the CVD process was confirmed using XPS, FTIR and Raman analysis. However, the peak intensity of the D band was reasonably high, indicating a high defect density. Therefore, the quality of the carbonaceous films coating needs to be improved in the future.

#### 4. Conclusion

An easy method of coating Cu nano powders with carbonaceous films using a solid carbon source was discussed. Using the polyol method, the copper nanopowder was coated with 10-nm-thick PVP during the synthesis of the copper nanoparticles. With CVD, the PVP is reduced to carbonaceous films via C–N bond breakage. The optimum process temperature and time were 900 °C and 2–3 min, respectively. Moreover, adding extra PVP solution blocked necking among the Cu nanoparticles during the conversion to carbonaceous films because the 10-nm-thick PVP layer alone is not thick enough to block necking. Adding extra PVP solution protected the copper nanopowder from agglomeration and oxidation in air. The optimum amount to reduce the agglomeration of Cu nanopowder, while minimizing the thickness of the coating, was 30 wt% PVP. TG-DTA, XPS, FT-IR and Raman analyses were used to confirm the conversion of PVP to carbonaceous films.

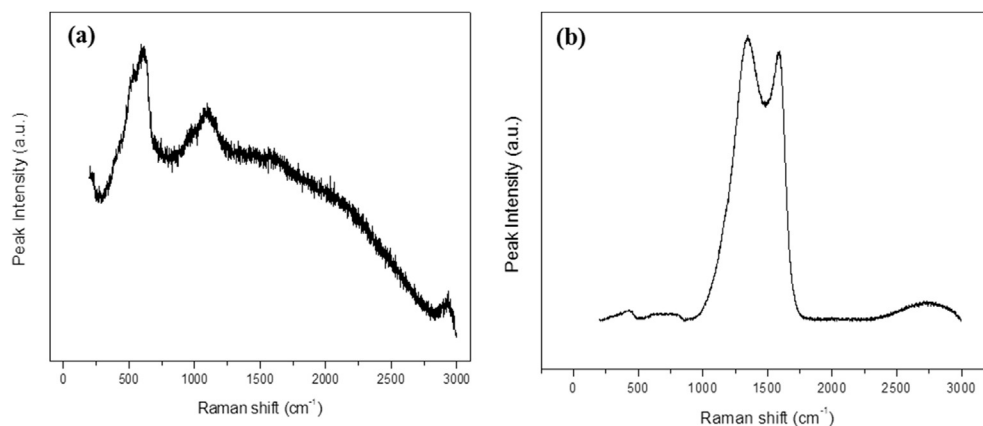


**Fig. 14.** Raman spectra of PVP-coated copper nanopowders with 30 wt% PVP solution (a) before and (b) after the CVD process (Table 1, sample No. 8).

## Acknowledgments

This work was supported by Basic Science Research Program through the National Research Foundation of Korea(NRF) funded by the Ministry of Education, Science and Technology (NRF-2012R1A1A3004290), by the National Research Foundation of Korea (NRF) grant funded by the Korea government (MEST) (No. 2012R1A2A2A01047189) and (No. 2013R1A1A2074605).

## References

- [1] D.J. Kim, J.H. Moon, *Electrochem. Solid-State Lett.* 8 (2005) J30–J33.
- [2] H.S. Kim, S.R. Dhage, D.E. Shim, H. Thomas Hahn, *Appl. Phys. A* 97 (2009) 791–798.
- [3] J.S. Kang, H.S. Kim, J. Ryu, H.T. Hahn, S. Jang, J.W. Jang, *J. Mater. Sci. Metal. Electron.* 21 (2010) 1213–1220.
- [4] J.S. Kang, J. Ryu, H.S. Kim, H.T. Hahn, *Electron. Mater.* 40 (2011) 2268–2277.
- [5] S.H. Koa, J. Chung, H. Pana, C.P. Grigoropoulos, D. Poulikakos, *Sens. Actuators A Phys.* 134 (2007) 161–168.
- [6] S. Magdassi, M. Grouchko, A. Kamysny, *Materials* 3 (2010) 4626–4638.
- [7] M. Grouchko, A. Kamysny, K. Ben-Ami, S. Magdassi, *J. Nanopart. Res.* 11 (2009) 713–716.
- [8] M. Cazayous, C. Langlois, T. Oikawa, C. Ricolleau, A. Sacuto, *Phys. Rev. B* 73 (2006) 113402.
- [9] K.H. Ng, R.M. Penner, *J. Electroanal. Chem.* 522 (2002) 86–94.
- [10] M. Grouchko, A. Kamysny, S. Magdassi, *J. Mater. Chem.* 19 (2009) 3057–3062.
- [11] D.E. Tallman, G. Spinks, A. Dominis, G.G. Wallace, *J. Solid State Electrochem.* 6 (2002) 73–84.
- [12] S. Jeong, K. Woo, D. Kim, S. Lim, J.S. Kim, H. Shin, Y. Xia, J. Moon, *Adv. Func. Mater.* 18 (2008) 679–686.
- [13] V. Engels, F. Benaskar, D.A. Jefferson, D.F.G. Johnson, A.E.H. Wheatley, *Dalton Trans.* 39 (2010) 6496–6502.
- [14] Y. Kobayashi, S. Ishida, K. Ihara, Y. Yasuda, T. Morita, S. Yamada, *Colloid Polym. Sci.* 287 (2009) 877–880.
- [15] P. Pulkkinen, J. Shan, K. Leppanen, A. Kansakoski, A. Laiho, M. Jarn, H. Tenhu, *ACS Appl. Mater. Interf.* 1 (2009) 519–525.
- [16] T.P. Ang, T.S.A. Wee, W.S. Chin, *J. Phys. Chem. B* 108 (2004) 11001–11010.
- [17] J.C. Huie, *Smart Mater. Struct.* 12 (2003) 264–271.
- [18] D. Prasai, J.C. Tuberquia, R.R. Harl, G.K. Jennings, K.I. Bolotin, *ACS Nano* 6 (2012) 1102–1108.
- [19] A.T. Lusk, G.K. Jennings, *Langmuir* 17 (2001) 7830–7836.
- [20] J. Her, D. Cho, C.S. Lee, *Mater. Trans.* 54 (2013) 599–602.
- [21] X. Du, I. Skachko, A. Barker, E.Y. Andrei, *Nat. Nanotechnol.* 3 (2008) 491–495.
- [22] C. Mattevi, H. Kima, M. Chhowalla, *J. Mater. Chem.* 21 (2011) 3324–3334.
- [23] L. Liu, S. Ryu, R. Michelle, E. Tomasik, N. Jung, M.S. Hybertsen, M.L. Steigerwald, L.E. Brus, G.W. Flynn, *Nano Lett.* 8 (2008) 1965–1970.
- [24] S. Chen, L. Brown, M. Levendorf, W. Cai, S. Ju, J. Edgeworth, X. Li, C. Magnuson, A. Velamakanni, R.D. Piner, J. Kang, J. Park, R.S. Ruoff, *ACS Nano* 5 (2011) 1321–1327.
- [25] K.S. Kim, Y. Zhao, H. Jang, S.Y. Lee, J.M. Kim, K.S. Kim, J.-H. Ahn, P. Kim, J.-Y. Choi, B.H. Hong, *Nature* 457 (2009) 706–710.
- [26] S.Y. Kwon, C.V. Ciobanu, V. Petrova, V.B. Shenoy, J. Bareno, V. Gambin, I. Petrov, S. Kodambaka, *Nano Lett.* 9 (2009) 3985–3990.
- [27] X. Li, W. Cai, J. An, S. Kim, J. Nah, D. Yang, R. Piner, A. Velamakanni, I. Jung, E. Tutuc, S.K. Banerjee, L. Colombo, R.S. Ruoff, *Science* 324 (2009) 1312–1314.
- [28] A. Earnshaw, T.J. Harrington, *The Chemistry of the Transition Elements*, Oxford University Press, 1972.
- [29] J.C. Hamilton, J.M. Blakely, *Surf. Sci.* 91 (1980) 199–217.
- [30] M. Eizenberg, J.M. Blakely, *Surf. Sci.* 82 (1979) 228–236.
- [31] A.N. Obraztsov, E.A. Obraztsova, A.V. Tyurnina, A.A. Zolotukhin, *Carbon* 45 (2007) 2017–2021.
- [32] A. Reina, X. Jia, J. Ho, D. Nezich, H. Son, V. Bulovic, M.S. Dresselhaus, J. Kong, *Nano Lett.* 9 (2009) 30–35.
- [33] M. Zheng, K. Takei, B. Hsia, H. Fang, X. Zhang, N. Ferralis, H. Ko, Y. Chueh, Y. Zhang, R. Maboudian, A. Javey, *Appl. Phys. Lett.* 96 (2010) 063110.
- [34] Z. Yan, Z. Peng, Z. Sun, J. Yao, Y. Zhu, Z. Liu, P.M. Ajayan, J.M. Tour, *ACS Nano* 5 (2011) 8187–8192.
- [35] Z. Peng, Z. Yan, Z. Sun, J.M. Tour, *ACS Nano* 5 (2011) 8241–8247.
- [36] S. Byun, H. Lim, G. Shin, T. Han, S. Oh, J. Ahn, H. Choi, T. Lee, *J. Phys. Chem. Lett.* 2 (2011) 493–497.
- [37] Z. Sun, Z. Yan, J. Yao, E. Beitler, Y. Zhu, J.M. Tour, *Nature* 468 (2010) 549–552.
- [38] S. Lee, J. Hong, J. Koo, H. Lee, S. Lee, T. Choi, H. Jung, B. Koo, J. Park, H. Kim, Y. Kim, T. Lee, *ACS Appl. Mater. Interf.* 5 (2013) 2432–2437.
- [39] K.J. Carroll, J.U. Reveles, M.D. Shultz, S.N. Khanna, E.E. Carpenter, *J. Phys. Chem. C* 115 (2011) 2656–2664.
- [40] Pattanawong Chokratanasombat, Ekasit Nisaratanaporn, *Eng. J.* 16 (2012) 39–46.
- [41] M.F. Silva, C.A. da Silva, F.C. Fogo, E.A.G. Pineda, Anita A.W. Hechenleitner, *J. Therm. Anal. Calorim.* 79 (2005) 367–370.
- [42] T. Agarwal, K.A. Gupta, S. Alam, M.G.H. Zaidi, *Int. J. Compos. Mater.* 2 (2012) 17–21.
- [43] Y.K. Du, P. Yang, Z.G. Mou, N.P. Hua, L. Jiang, *J. Appl. Polym. Sci.* 99 (2006) 23–26.
- [44] B. Park, S. Jeong, D. Kim, J. Moon, S. Lim, J. Kim, *J. Colloid Interf. Sci.* 311 (2007) 417–424.
- [45] J. Chrzanowski, J.C. Irwin, *Solid State* 70 (1989) 11–14.
- [46] P. Colomban, H.D. Schreiber, *J. Raman Spectrosc.* 36 (2005) 884–890.
- [47] Z. Ni, Y. Wang, T. Yu, Z. Shen, *Nano Res.* 1 (2008) 273–291.
- [48] C. Thomsen, S. Reich, *Phys. Rev. Lett.* 85 (2000) 5214–5217.
- [49] S. Reich, C. Thomsen, *Philos. Trans. R. Soc. Lond. A* 362 (2004) 2271–2288.
- [50] M.S. Dresselhaus, P.C. Eklund, *Adv. Phys.* 49 (2000) 705–814.
- [51] M.S. Dresselhaus, G. Dresselhaus, R. Saito, A. Jorio, *Phys. Rep.* 409 (2005) 47–100.
- [52] P.K. Chu, L. Li, *Mat. Chem. Phys.* 96 (2006) 253–277.
- [53] H.A. Becerril, J. Mao, Z. Liu, R.M. Stoltenberg, Z. Bao, Y. Chen, *ACS Nano* 2 (2008) 463–470.
- [54] N.T. Dung, N.V. Khoa, J.-M. Herrmann, *Int. J. Photoenergy* 7 (2005) 11–15.
- [55] Z. Guangxia, Z. Qiaoyun, C. Zemin, in: *Third International Conference on Digital Manufacturing & Automation*, 2012, 2012, pp. 521–523.
- [56] J. Jays, A. Kumar, C.H.S. Venketaramana, B.V. Sumaa, V. Madhavan, *Int. J. ChemTech Res.* 3 (2) (2011) 772–777.
- [57] N.L. Prasanthi, S.S. Manikiran, N. Rama Rao, *Arch. Appl. Sci. Res.* 3 (2011) 513–519.
- [58] H. Wang, X. Qiao, J. Chena, X. Wang, S. Ding, *Mater. Chem. Phys.* 94 (2005) 449–453.
- [59] Y. Guo, X. Sun, Y. Liu, W. Wang, H. Qiu, J. Gao, *Carbon* 50 (2012) 2513–2523.
- [60] M.R. Johan, M.S.M. Suan, N.L. Hawari, H.A. Ching, *Int. J. Electrochem. Sci.* 6 (2011) 6094–6104.